International Journal of Advanced Manufacturing Technology, Vol. 93, Issue 9-12, December 2017, pp. 4007-4013
DOI:10.1007/s00170-017-0829-5

A hybrid cellular automata – finite elements model for the simulation of the grind-hardening process

Konstantinos Salonitis

Manufacturing Department, Cranfield University, Bedford, UK

B50, College Road, MK430AL, UK

E: k.salonitis@cranfield.ac.u

T: +44(0)1234 758347

Abstract

Grind-hardening process is a hybrid process for the simultaneous finishing and heat-treatment of the workpiece material. Several studies have been presented for the simulation of the process, using either analytical or finite element based models. In the present paper, the cellular automata method is used for simulating the metallurgical changes in the workpiece material. The method is coupled with a finite elements model for the macro-modelling of the process, allowing the prediction of the microstructure of the material as a function of the macro-process parameters.

Keywords

Grinding; Modelling; Surface hardening; cellular automata

1. Introduction

Grind-hardening process has a short history compared to other well-research abrasive processes. It was introduced within CIRP community by Brinksmeier and Brockhoff in 1996 [1]. A brief and comprehensive description of the process would be that grind-hardening is a hybrid process that combines material removal and surface hardening of the workpiece at the same time [2]. The basic mechanism behind the process relies on the heat dissipation within the grinding zone for the heat treatment of the workpiece. Heat is generated in the interface between the grinding wheel and the workpiece material, resulting locally in the rapid heating of the material. The metallurgic change required for hardening is achieved in two steps; heating the workpiece surface above the austenitization temperature, and afterwards quenching the material for inducing martensitic transformation.

The process has been the focus on several studies in the last 20 years. A thorough review of the state of the art of grind hardening process studies was published recently [2]. However, no studies have been presented on the microstructure induced by the grind-hardening process. The characteristics of the produced microstructures are influenced by many factors, among which are the heat input rate, the cooling rate, the material properties etc. The heat input rate is a function of the process parameters (cutting speed, depth of cut and feed speed) and the characteristics of the grinding wheel. Similarly, the cooling rate is a function of the coolant fluid application and the material properties [3, 4]. The properties of the material affect the dissipation of the heat within the workpiece. The hardening capability of any workpiece material is a function of the chemical composition and the microstructure of the material. This limits the applicability of the process to specific materials such as martensitic hardenable steels. The hardening result is determined by the carbon content and the content of alloying elements.

Majority of the modelling studies presented in the literature are using the finite element analysis (FEA) method for the prediction of the temperature distribution [3,4] and residual stress accumulation [5,6]. There is a sparse literature on the modelling of microstructure for grind-hardening process. As indicated by Brinksmeier et al. [7], the modelling of the workpiece material microstructure due to grinding processes is performed using molecular

dynamics (MD). However, there are limitations with such an approach with the most important one being the maximum size of the model. The analysis of grinding process using MD is restricted to few grits engaging with the workpiece material. This modelling problem can be approached by using the Cellular Automata (CA) modelling technique. CA is a discrete modelling method that consists of a grid of cells, each one of a finite number of states. Using such an approach, each material grain can be modelled as cells with rules that characterize their state. This approach has been used for modelling the grain structure resulting from other processes, such as laser additive manufacturing [8] and induction hardening [9] but never before for an abrasive process such as grind-hardening.

The present paper proposes a hybrid model using FEA and CA for the simulation of grind-hardening process. It discusses the effect of key parameters identified by the proposed model on the microstructure resulting from the process.

2. Process physics and modelling framework

Grind hardening process uses the heat generated in the grinding zone for the surface hardening of the workpiece material. The surface hardening is a result of metallurgical changes in the material structure. The hardening mechanism is based on the phase transformation of austenite to martensite that occurs during the quenching of the material after the grinding has taken place. The workpiece material before any heat treatment process has ferritic–perlitic structure. During the process, heat is generated mainly due to friction in the interface between the grinding wheel and workpiece material. Thus, heat flows from the contact zone into the workpiece, resulting in the increase of the surface temperature. When the temperature exceeds a critical temperature, the carbides in the lamellar pearlite begin to dissolve into iron formatting austenite lattices. As the temperature increases, more carbides are dissolved until the steel consists completely of austenite.

This crystal structure is characterized by higher strength, but cannot be sustained in ambient temperatures. For “locking” this structure, austenite must be transformed to martensite. This is achieved by rapid cooling of the workpiece material (quenching) that stops the diffusion-dependent transformation that would transform austenite back to ferrite–pearlite structure.

The cooling rate is the critical parameter to be controlled for achieving the desired micro-structure. This is a function of the cooling mechanism, the carbon content of the workpiece material and of the holding time above the austenization temperature. For the case of grind hardening, the required cooling is achieved through heat dissipation from the austenitized surface layer to the cooler workpiece material volume (characterized as self-quenching) and/or by using a coolant fluid.

A key step in the simulation of the process is the calculation of the temperature field. This can be easily achieved through a FEA model; however, it requires the description and modelling of the heat transfer between the various heat sinks (in the case of grind-hardening these are the grinding wheel, the workpiece material, the chips, the coolant fluid and the environment). For modelling and predicting the microstructure, a CA model is used afterwards.

The modelling approach thus includes the following three steps: (i) analytical calculation of the heat generated and transferred to the workpiece material, (ii) calculation of the temperature field using FEA and (iii) modelling of the micro-structure evolution using CA simulation. Step (i) is performed only in the start of the modelling for calculating the average heat input entering the workpiece material. Steps (ii) and (iii) are repeated for each time step to simulate the feed of the grinding wheel on the workpiece. This simulation approach is shown in fig. 1. Each step modelling is presented in more detail in the following sections.

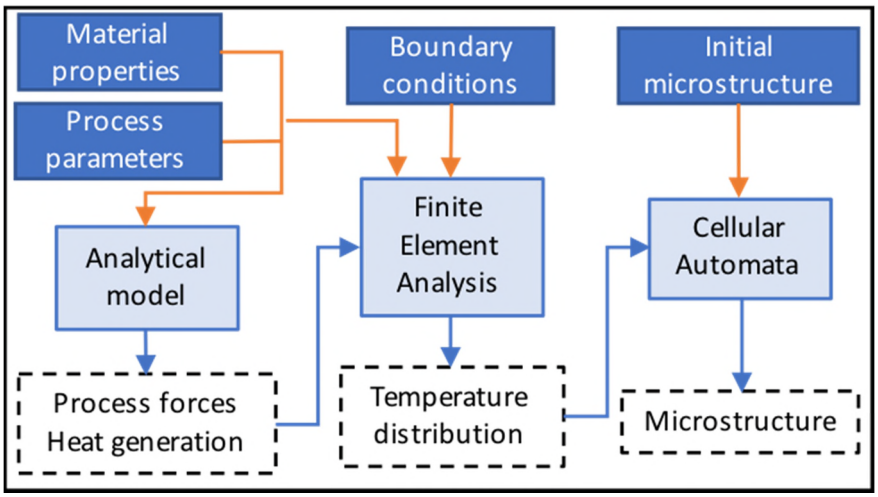

Figure 1. Schematic of simulation approach

3. Model development

3.1. Analytical modelling

The heat generation mechanism and the partition of the heat to the various heat sinks has been investigated theoretically in several studies [3-4]. The heat generated during the process equals the grinding wheel spindle power and can be estimated from the tangential component of the cutting forces. The cutting forces depend on the process parameters (depth of cut, a_e, cutting speed, u_s, and feed speed u_w), the grinding wheel topography, and the workpiece material. They can be calculated either analytically [10] of empirically [11]. Both methods have been used successfully in the past. In the present study, the empirical calculation was selected due to its simplicity and relatively easy determination of the model's coefficients.

The fraction of the heat generated that is absorbed by the workpiece can be estimated using the simplified heat partition model developed by Rowe et al. [12]. At typical grind-hardening workpiece speeds, the heat partition to the grinding wheel is in the range of 35–55 % whereas the heat partition to the workpiece is in the range of 40–60 % [3-6].

3.2. Finite element modelling

Following the usual strategy in such problems, the grinding wheel is substituted by a moving heat source sliding on the workpiece material. The process and finite element model are shown in fig. 2. The heat source distribution is assumed to present triangular distribution over the contact length, with its peak being at the direction of movement. Due to the high depth of cuts (0.3 to 1.0 mm), the contact length is simulated as an arc. The removal of the upper layer is also modelled through the birth and death of the finite elements. Initially, all the elements are "alive". In each time step, a number of elements that are corresponding to the heat source (the arc that is shown in red in figure 2.b) are "loaded" with heat input (simulating the heat transfer occurring between the grinding wheel and the workpiece material). Once the elements are "loaded" with heat, in the next time step they are disabled ("dead").

The messing of the geometry is quite simple, and based on the results of the finite element model, the upper layer of the remaining ground workpiece where temperature exceeds 75% of the austenitization temperature is modelled using CA. The models employ square meshes (with different resolution though, the FEA elements are of 0.5 mm length, whereas the CA cells are of 2μm) and the same time step.

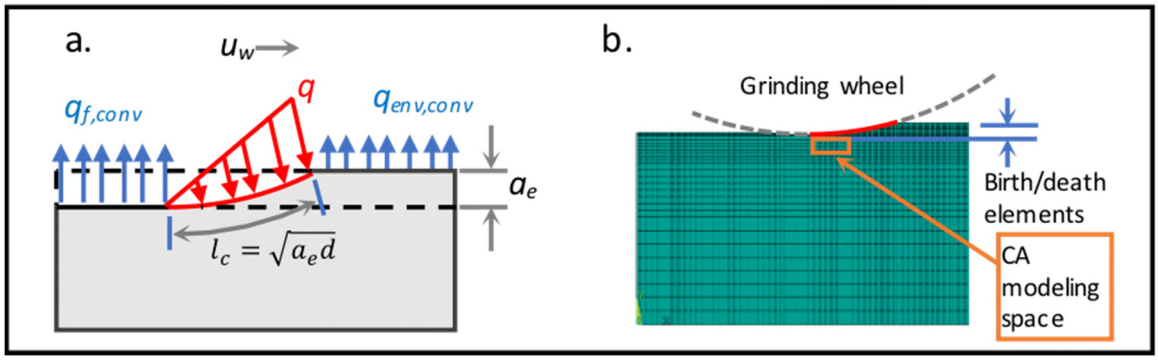

Figure 2. (a) Process and (b) finite element models (meshing simplified)

3.3. Cellular automata modelling

The CA method is used for simulating many problems in different sectors such as mathematics, biology, computer science etc. [13]. A CA model consists of a grid of cells, with each one having a finite number of states. For the needs of the present paper, each cell has a specific phase indicating its crystalic structure (ferrite/perlite, austenite, retained austenite, martensite) and is characterized by its temperature and an index defining the cell belonging to a specific grain. For every time step, the state of each cell is calculated as a function of the state of the neighbouring cells, affecting the future state of the cells in its neighbourhood as well. Each cell can belong to only one grain, and thus the grain boundary cells can be identified. As per Bos et al. [14], each time step, *t*, the growth length, l^i_{cell}, for every grain-boundary cell, *i*, is calculated. The following simple equation is used:

$$l^i_{cell}(t + \Delta t) = l^i_{cell}(t) + u^i_{cell}(\Delta t) \quad (1)$$

with u^i_{cell} being the grain boundary velocity that can be calculated when the phase transition type is known (for example from ferrite/pearlite to austenite). The same rules that have been

introduced by Bos et al. [14] with regards the grains' growth are used, and the reader is suggested to refer to their study for more information.

Identifying the rules of transformation for each cell is critical for using CA, and the number of rules that need to be established is un-realistic for a deterministic solution, since this is a function of the number of neighbour cells considered and the number of different states. For this reason, in the present paper the state of each cell is probabilistically estimated based on the temperature history (maximum temperature, holding time, cooling rate, undercooling etc.) of each cell. The Moore configuration is used to define the neighbourhood. The CA cells form grains that grow over time. Their growing is defined by the grain-boundary velocity, that is estimated by the following equation:

$$u = M\Delta G \quad (2)$$

where u is the grain-boundary velocity and ΔG is the driving force for the transformation.

To simplify the model and reduce the computation time, the CA model takes place in two phases, thus sub-models are used that describe each phase. The first phase focuses on the rapid heating of the workpiece material, where the initial microstructure (ferrite/perlite) is transformed into austenite, and the second phase focusses on the quenching with austenite transforming into martensite. These two phases are governed by different rules and mechanisms, as the ferrite/perlite transformation to austenite takes place through diffusion whereas the austenite to martensite transformation is diffussionless. For the modelling of the heating phase, the approach proposed by Bos et al. [14] was adopted. The austenite grains nucleation is initiated when a critical temperature is reached. During grind-hardening the heating rate is high, resulting in the increase of the critical temperature. When the critical temperature is reached, austenite nucleation and grain growth will occur simultaneously. This critical temperature can be estimated based on the approach presented by Salonitis and Chryssolouris [3]. Due to temperature gradients in the workpiece during heating, austenitization occurs at different rates at different locations, so the microstructure and the grain size distribution will be non-uniform. In the present study, the growing of austenite grains is modelled as in [14] based on interface-controlled model. The critical temperature for the onset of the nucleation and grow of austenite grains is calculated based on [9].

Nucleation of austenite grains is described as site-saturation; which can be interpreted as a collection of pre-existing nuclei that start to grow when a certain temperature is reached. In the CA-model this is implemented as a nucleation density and a nucleation temperature, which are input parameters as suggested in [14]. The growth kinetics thus are described with the following equation (expressing the grain boundary velocity):

$$u = M_0^{\gamma P} exp\left(-{Q_g^{\gamma P}}/{RT}\right)\Delta G_{\gamma P} \quad (3)$$

in this case thus, as suggested by Bos et al. [14] the pearlite transforms in a small temperature range, and thus pearlite to austenite force $\Delta G_{\gamma P}$ is considered a constant. Both pearlite and ferrite in the present study are treated as pearlite for their transformation to austenite. All values in the equation ($\Delta G_{\gamma P}$, pre-factor $M_0^{\gamma P}$ and activation energy $Q_g^{\gamma P}$) are input parameters and have to be assumed.

The martensitic transformation, as indicated, is a diffusionless phase change. For the modelling of this transformation an indirect approach was decided. The model is set to simulate the diffusion transformation of austenite back to ferrite and perlite, however due to the excessive cooling rates and the undercooling, the diffusion is limited and most of the austenite is crystalized into a phase that is a mix of retained austenite and martensite. Using the Koistinen–Marburger model [15], the ratio of martensite formation to austenite retention can be determined locally as a function of undercooling, using the following equation:

$$f = 1 - e^{-0.011\Delta T} \quad (4)$$

where f is the volume fraction of martensite and ΔT is the undercooling below the martensitic onset temperature.

3.4. FEA and CA models integration

The two models do not share the same meshing. Each finite element corresponds to 250x250 CA cells. The transfer of results between the two models is based on a simple approach:

- each finite element is divided into 250x250 virtual elements (each virtual element coincides with a CA cell)
- the finite element temperature and cooling rate calculated at the nodes is interpolated to the virtual nodes of each virtual element using bilinear interpolation

- the temperature of each CA cell is calculated as the average temperature of the four virtual nodes temperature

Initially the cells corresponding to the finite element, are all characterized by a uniform temperature. However, after each finite element analysis step run, the cells temperature is calculated as described previously. The cell phase changes when and where the temperature crosses the critical temperature for each phase (austenitization temperature, martensitic etc). The modelling was implemented by using ANSYS for the FEA model and Mathematica 10 for the CA model. The link between the FEA data output (elements' temperature, cooling rate etc.) and the CA input is through a VBA routine within Microsoft Excel that runs the bilinear interpolation.

4. Feasibility Study

As a feasibility study, the grind-hardening process for the case of AISI 1045 was simulated. After calculating the heat generated in the interface with the grinding wheel, and the portion of the energy dissipated to the workpiece material; the FEA model was run and the temperature distribution and history were calculated (fig. 3). The FEA model settings and material properties used for the calculations are described in detail in [5]. Subsequently, the CA model is to be used for the simulation of the resulting microstructure. The configurations of the CA model (i.e. the initial state that each cell poses) was generated as a random ferrite/perlite structure (fig. 4). Since the material microstructure presents stochasticity, a VBA module was developed for the random generation of the material microstructure before the grind-hardening process. The input to this module is the expected average grain size and its standard deviation. The CA model was run for a big number of different random configurations (following a Monte-Carlo approach) to estimate the converged final microstructure characteristics. In fig. 5, the results of one of these runs are shown.

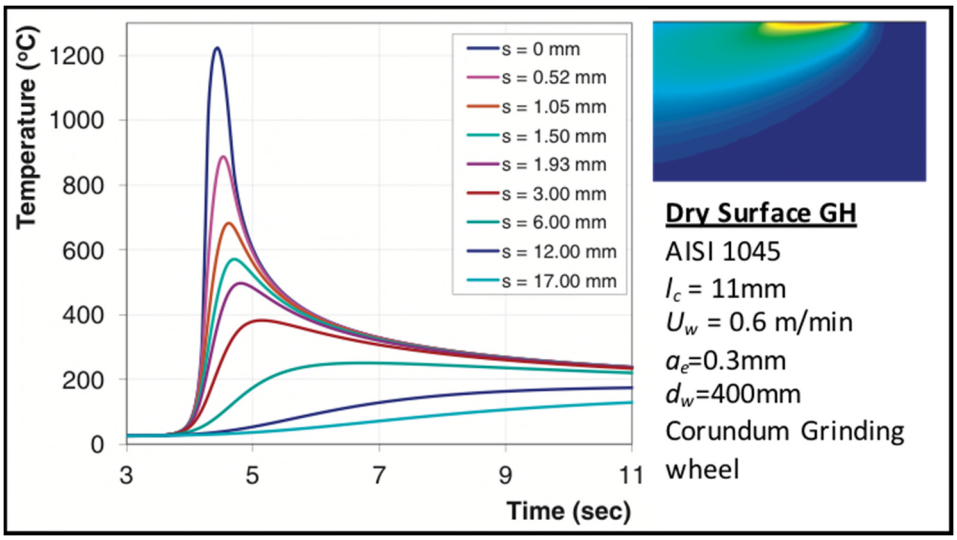

Figure 3. Temperature distribution and history as a function of depth from the workpiece surface

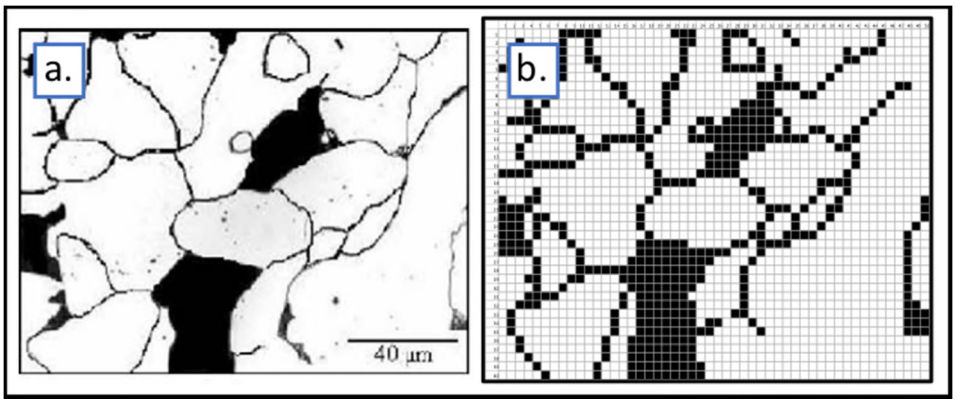

Figure 4. CA configuration: (a) a ferrite-perlite example microstructure [16], (b) approximated microstructure comprising of CA objects

Based on these results, the model can be validated. Martensite grain is predicted from the surface up to a depth of 0.3mm. This agrees to the experimental results, where the hardness penetration depth was measured to be 0.34mm. Furthermore, the concentration of retained austenite close to the surface (up to 40 μm from the surface) is higher to the rest of the hardened depth. This is also in agreement with the prediction of Koistinen–Marburger model [15]. Finally, for steel with greater than 1% carbon, the martensite is expected to form a plate like structure, as is predicted in fig. 4 for AISI 1045. This was further investigated; the CA model was run with finer cell sizes to capture lath structures in case this was not possible with the 2μm size cell. The model also predicts a transition phase (area C in fig. 5), where the microstructure is a mix of martensite, retained austenite and ferrite/perlite, with the latter being the predominant phase as we move away from the hardened area. This was also

evidenced in the experimental result with the micro-hardness dropping almost linearly in this area.

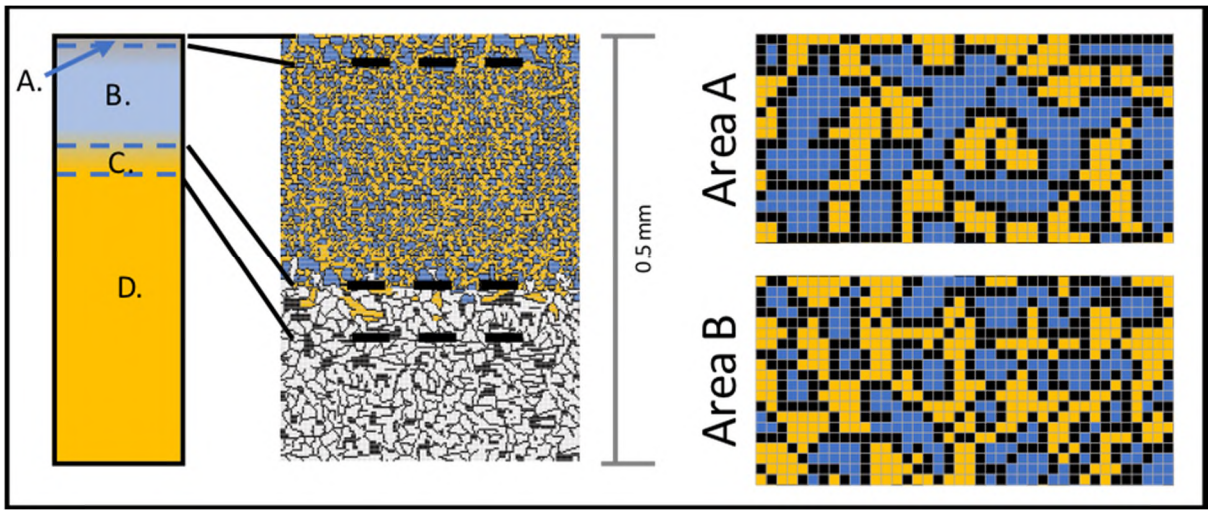

Figure 5. Cellular automata results

5. Results and discussion

The use of such a simulation tool can allow the prediction of the finished part microstructure, and tailor the process as to develop desirable characteristics. The key microstructure characteristics that should be controlled are the grain size and the composition of the various phases.

The grain size is critical and affects the brittleness of the material. Both the heating and the cooling phases affect the microstructure. The austenitization process takes place above the critical-temperature, and initially small grains of austenite form. However, the overheating of the material results in larger austenite grains, and as shown in fig. 3, overheating by up to 400^{o}K is observed close to the material surface. Subsequently, during the quenching, the austenite grain-size directly affects the martensitic grain-size. Larger grains have large grain-boundaries, which serve as weak spots in the structure. Using the model developed, the distribution of the grain size can be calculated for different depths. The grain size of martensite drops by ca. 25% after 30μm, and stays relatively constant till the end of the hardened depth. In fig. 6 the size of martensite grains as a function of distance from the surface, as well the distribution at two different distances, are presented. A practical

implication of this result is that at least 40μm need to be removed through finish grinding after grind-hardening, for improving the mechanical performance of the part. The simulation was also run for the case of grind-hardening with the assistance of coolant fluid for enhancing the quenching (wet grind-hardening). The simulation indicated similar grain sizes in all regions, however, the first region (Area A in fig. 5) was smaller in length (20μm) and the hardened zone was considerably deeper (from 0.30 to 0.42mm). The former can be justified since the use of coolant fluid reduces slightly the peak temperature and thus austenitization happens with lower overheating, resulting in finer grains. The latter is due to the higher cooling rate, allowing deeper areas to reach the martensitic transformation temperature before the total diffusion of austenite to perlite and/or ferrite.

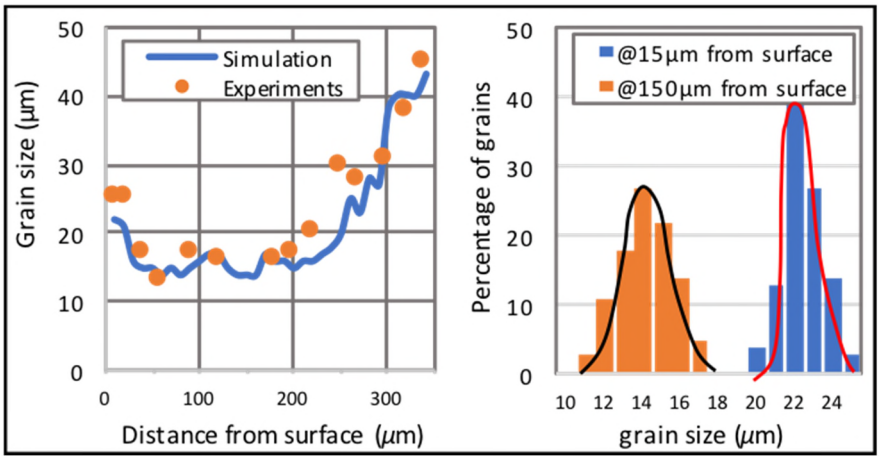

Figure 6. Martensitic grain size distribution

In Fig. 7, the evolution of the phase transformations for the case of wet grind-hardening is presented. The two critical areas are highlighted. During the austenitization phase, ferrite and perlite are transformed into austenite through diffusion. Once the temperature drops below the critical austenitization temperature (A_c), austenite starts to diffuse back to ferrite/perlite structures. Only when the temperature drops below the critical martensitic onset temperature (M_S), the difussionless transformation of austenite to martnesite will begin. Thus, the longer it takes to drop temperature from Ac to Ms, the less austenite will be available to transform to martensite. In fig. 7, for the process parameters combination, it takes about 2 secs, for the case of dry grind-hardening the cooling takes 10 secs, further justifying the difference in the hardness penetration depth.

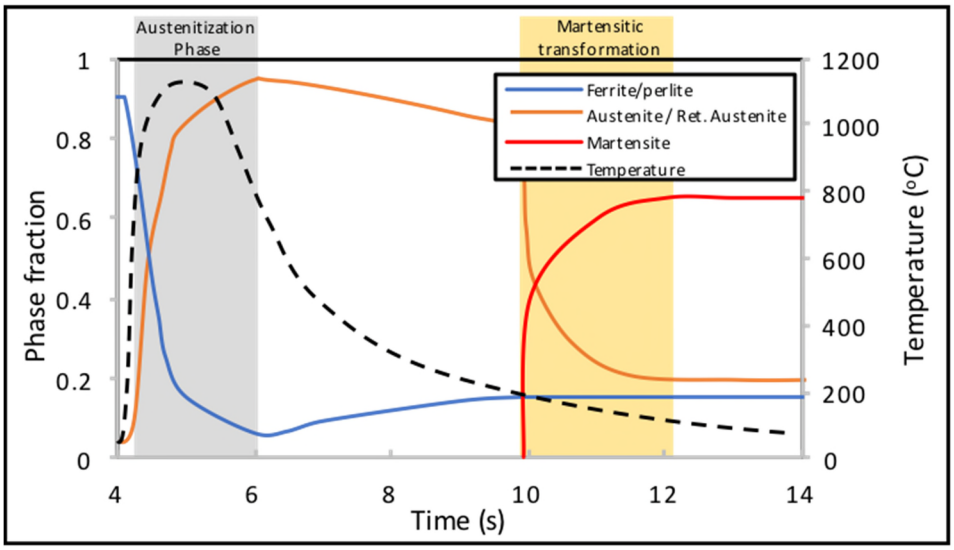

Figure 7. Phase fraction prediction and temperature evolution for the case of wet grind-hardening at 0.15mm from the workpiece surface (a_e=0.3mm, u_w=0.6m/min)

Based on the calculated phase distribution, the micro-hardness can be estimated locally, following the approach proposed by Leslie [17]. In fig. 8, the calculated and the experimentally determined micro-hardness are shown for wet and dry grind-hardening. The experimental results reveal and confirms the phases identified in figure 5. The hardness reaches the maximum achievable value (750 HV) within 20 to 40µm from the surface, depending on whether the process takes place under wet or dry conditions. Hardness starts reducing to the hardness expected for a perlitic structure after 0.3 for dry and 0.4mm for wet grind-hardening. As explained, this is due to the lower cooling rates, resulting in the transformation of austenite back to perlite/ferrite.

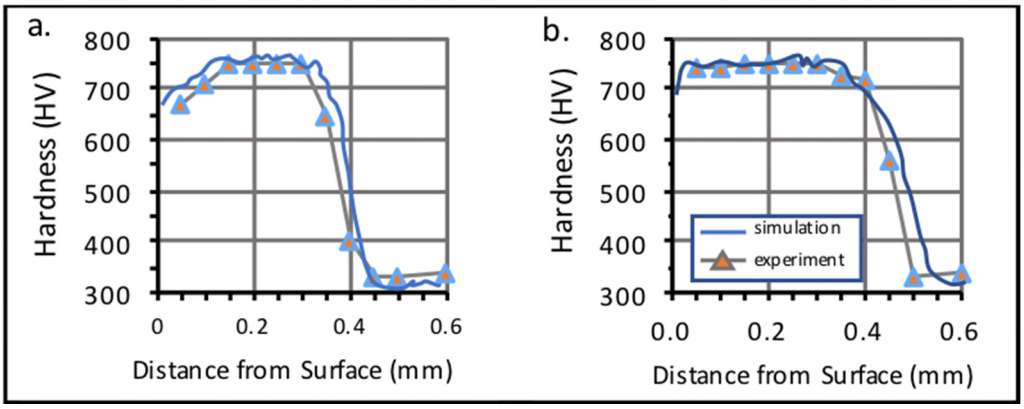

Figure 8. Hardness profile for a. dry and b. wet grind-hardening

6. Conclusions

A hybrid model for predicting the micro-structure evolution resulting from the grind-hardening process has been developed using FEA and CA. The following conclusions can be derived:

(1) The CA method is very effective for simulating the phase transformation, visualization of the phase changes and revealing the phase changes locally
(2) The simulation allowed for better understanding of the microstructure phase changes during the process, identifying the critical aspects that need to be controlled
(3) The simulation can be used for better programming offline the grind-hardening process

Finally, few practical implications for the application of grind-hardening can be also suggested based on the simulations:

(1) Post process, a finishing grinding (20-40μm) is suggested for removing material close to the surface that exhibit microstructure with larger grains
(2) The use of coolant fluid for assisting the quenching phase, increases the hardness penetration depth and slightly reduces the grain size of martensite.

The next steps of this study will be integration of the three tools (ANSYS model, CA model and VBA for the linking of the two) and combining them with optimization algorithm for selecting process parameters and grind-hardening settings for achieving specific product characteristics.

References

[1] Brinksmeier E, Brockhoff T (1996) Utilization of grinding heat as a new heat treatment process. CIRP Ann Manuf Technol 45(1):283–286

[2] Salonitis K (2015) Grind hardening process, Springer International Publishing: Cham, Heidelberg

[3] Salonitis K, Chryssolouris G (2007) Cooling in grind-hardening operations. Int J Adv Manuf Technol 33(3):285–297

[4] Salonitis K, Chrondros T, Chryssolouris G (2008) Grinding wheel effect on grind-hardening process. Int J Adv Manuf Technol 38(1):48–58

[5] Salonitis K, Kolios A (2015) Experimental and numerical study of grind-hardening induced residual stresses on AISI 1045 Steel. Int J Adv Manuf Technol 79(9): 1443–1452

[6] Salonitis K. (2014) On Surface Grind Hardening Induced Residual Stresses. Procedia CIRP 13: 264–269

[7] Brinksmeier E et al. (2006) Advances in Modeling and Simulation of Grinding Processes. CIRP Ann Manuf Technol 55(2):667-696

[8] Zinoviev A et al. (2016) Evolution of grain structure during laser additive manufacturing. Simulation by a cellular automate method. Materials and Design 106:321-329

[9] Yang BJ et al. (2010) Simulation of steel microstructure evolution during induction heating. Materials Science and Engineering: A 527(12): 2978–2984

[10] Salonitis K, Stavropoulos P, Kolios A (2014) External grind-hardening forces modelling and experimentation. Int J Adv Manuf Technol 70:523–530

[11] Toenshoff HK, Peters J, Inasaki I, Paul T (1992) Modelling and simulation of grinding processes. CIRP Ann Manuf Technol 41(2):677–688

[12] Rowe WB, Morgan MN, Black SCE (1998) Validation of thermal properties in grinding, Annals of the CIRP, 47(1):275- 279

[13] Wolfram S (2002). A New Kind of Science. Wolfram Media. ISBN:978-1579550080

[14] Bos C, Mecozzi MG, Sietsma J (2010) A microstructure model for recrystallisation and phase transformation during the dual-phase steel annealing cycle. Computational Materials Science 48(3):692-699

[15] Koistinen DP, Marburger RE (1959) A general equation prescribing the extent of the austenite-martensite transformation in pure iron-carbon alloys and plain carbon steels. Acta Metallurgica 7(1):59-60

[16] Das S (2010) Modelling mixed microstructures using a multi-level cuellular automata finite element framework. Computational Materials Science 47:705-711

2017-08-01

A hybrid cellular automata-finite element model for the simulation of the grind-hardening process

Salonitis, Konstantinos

Springer

Konstantinos Salonitis. A hybrid cellular automata-finite element model for the simulation of the grind-hardening process. International Journal of Advanced Manufacturing Technology, Vol. 93, Issue 9-12, December 2017, pp. 4007-4013

https://dspace.lib.cranfield.ac.uk/handle/1826/12411